

Supertetrahedral and Bi-supertetrahedral Cages: Synthesis, Structures, and Magnetic Properties of Deca- and Enneadecametallic Cobalt(II) Clusters**

Laurent Lisnard, Floriana Tuna, Andrea Candini, Marco Affronte, Richard E. P. Winpenny, and Eric J. L. McInnes*

Significant interest has arisen, owing to the detection of slow magnetic relaxation in single-molecule magnets (SMMs),^[1] where magnetic anisotropy arises from zero-field splitting of a large spin ground state. Slow relaxation in SMMs is rarely seen at temperatures above 1.8 K, and, even after two decades of study, the highest blocking temperatures (below which slow relaxation is observed) remain at around 4 K.^[2] Recently, we observed slow relaxation at 17 K in a {Ni₁₀} cage complex,^[3] which led us to propose a quite different mechanism to account for slow relaxation in the absence of any significant energy barrier from either high anisotropic spins (as in SMMs) or intermolecular interactions.

The {Ni₁₀} clusters possess a supertetrahedral core,^[4] incorporating Ni^{II} ions on the vertices and edges of a tetrahedron (Figure 1), centred on a μ_6 oxide, with trisalkoxide ligands^[5] binding the {Ni₆} faces. This topology leads to a magnetic structure consisting of dense, well-separated bands. There is strong antiferromagnetic coupling ($2|J| \approx 120 \text{ cm}^{-1}$) between the pairs of edge-Ni^{II} ions, which define an inner octahedron centred around the μ_6 oxide, and very weak coupling between the four vertex Ni ions, which define the outer tetrahedron. The result is a lowest-energy “band” consisting of $(2s + 1)^4 = 81$ levels, separated by approximately 120 cm^{-1} from the first excited band. This band structure requires both the highly frustrated topology and the weak magnetic coupling between vertex sites. Magnetic relaxation requires that low-energy phonons are dissipated into the lattice. However, in the model proposed for {Ni₁₀}, the existence of 81 levels within the lowest-energy band makes it much more probable that the phonons are reabsorbed by a neighboring molecule, and hence trapped, leading to slow relaxation at relatively high temperatures compared with SMMs. This mechanism was initially proposed

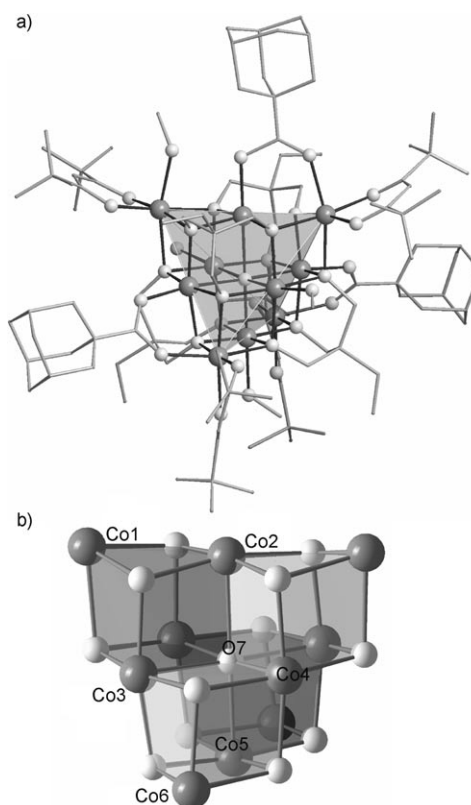


Figure 1. a) Structure of **1** in the crystal, with supertetrahedron highlighted; b) the {Co₁₀O₁₃} fused-heterocubane core (Co dark gray, O light gray, C skeleton only, H omitted for clarity).

by Anderson for relaxation in paramagnetic salts at low temperature,^[6] but not at high temperatures, as in {Ni₁₀}.

To test this theory, we required new materials, perhaps with the same topology^[7] but with different values for either the local spin s or the exchange J . Although such isomorphous high-nuclearity structures are very rare, a limited number of examples, incorporating nickel or cobalt, are known^[8–10] and, therefore, this target seemed achievable. Herein, we show that the Co^{II}–triol solvothermal reaction system is much more versatile than its Ni^{II} equivalent, with minor changes in reaction conditions leading to structurally related species including a symmetrical {Co^{II}₁₀} supertetrahedron, an opened, unsymmetrical {Co^{II}₁₀} supertetrahedron, and a vertex-sharing {Co^{II}₁₉} bi-supertetrahedron. Crucially, the symmetrical {Co₁₀} complex exhibits qualitatively similar magnetic behav-

[*] Dr. L. Lisnard, Dr. F. Tuna, Prof. R. E. P. Winpenny, Prof. E. J. L. McInnes
School of Chemistry, The University of Manchester
Oxford Road, Manchester M13 9PL (UK)
Fax: (+44) 161-275-4616
E-mail: eric.mcinnnes@manchester.ac.uk
Dr. A. Candini, Prof. M. Affronte
CNR-INFM-S3 NRC, Università di Modena e Reggio Emilia
Modena, I-41100 (Italy)

[**] This work was supported by the EPSRC (UK), the EC “Network of Excellence” MAGMANet, and the EC-TMR Network “QuEMolNa”.

Supporting information for this article is available on the WWW under <http://dx.doi.org/10.1002/anie.200804147>.

ior to $\{\text{Ni}_{10}\}$, whereas the unsymmetrical form does not, which supports the proposed model.

Reaction, in 1:1:1 stoichiometry, of $[\text{Co}(\text{dpm})_2(\text{H}_2\text{O})_2]$ (Hdpm = dipivaloylmethane), H_3tmp [1,1,1-tris(hydroxymethyl)propane, $\text{EtC}(\text{CH}_2\text{OH})_3$], and adamantyl carboxylic acid (AdCO_2H) in MeOH at 150°C yields $[\text{Co}_{10}\text{O}(\text{dpm})_4(\text{tmp})_4(\text{AdCO}_2)_2(\text{AdCO}_2\text{H})_{0.5}(\text{MeOH})_{3.5}(\text{H}_2\text{O})_{1.5}]$ as brown crystals (**1**; 51 %).^[11] The core consists of four edge-sharing $\{\text{Co}_4\text{O}_4\}$ cubane structures, centred around a μ_6 oxide (O7 in Figure 1b). The metal ions define a tetrahedron with each $\{\text{Co}_6\}$ face bound by a fully deprotonated $(\text{tmp})^{3-}$ ligand (6.333 binding in Harris notation^[12]) and diketonates chelating the vertices. Two carboxylate groups form bridges between Co3 and Co6, and between their symmetry equivalents Co3A and Co6A, and one bridging carboxylic acid disordered with solvent over Co1, Co2, and Co1A. Co4, Co4A, and Co5 have terminal solvent and all metal ions are six coordinate. Bond valence sums (BVS) and charge balancing indicate the presence of ten Co^{II} ions and one protonated acid (see the Supporting Information). Hence, the $\{\text{Co}_{10}\text{O}(\text{L})_4(\text{diketonate})_4\}$ core of **1** (L = fully deprotonated triol) is analogous to that of $\{\text{Ni}_{10}\}$.

The structure of the cobalt cluster product is sensitive to changes in ligands and solvent. For example, the use of the more constrained, cyclohexane-based triol H_3cht (H_3cht = *cis,cis*-1,3,5-cyclohexanetriol), in place of H_3tmp , results in a distorted $\{\text{Co}_{10}\}$ cage. The reaction of $[\text{Co}(\text{dpm})_2(\text{H}_2\text{O})_2]$ with H_3cht and AdCO_2H (1:1:1) in EtOH at 150°C affords $[\text{Co}_{10}\text{O}(\text{OH})(\text{dpm})_4(\text{cht})_2(\text{Hcht})_2(\text{AdCO}_2)_3(\text{EtOH})_3]$ (**2**; 66 %; Figure 2) as purple crystals.^[11] In this case, one of the four edge-sharing $\{\text{Co}_4\text{O}_4\}$ cubanes has a missing edge, and the supertetrahedron has an opened face (that incorporating Co1–5,10; Figure 2b). Two of the $\{\text{Co}_6\}$ faces are bound (6.333 binding in Harris notation^[12]) by fully deprotonated $(\text{cht})^{3-}$ ligands. The remaining two $\{\text{Co}_3\}$ faces are bound by monoprotonated $(\text{Hcht})^{2-}$ ligands, which have “slipped” towards edges, (5.331 binding in Harris notation^[12], Figure 2c). The remaining coordination sites on the open face are taken up by a monodentate carboxylate linking Co4 and Co10, and a μ_3 -hydroxide bridging Co5, Co9, and Co10. The two remaining carboxylate groups bridge Co9 and Co10, and terminally coordinate to Co5. Co1, Co3, and Co8 are each coordinated by a terminal solvent molecule, while Co4, Co5, and Co7 are five-coordinate. BVS and charge balancing support the presence of ten Co^{II} centers and one hydroxide ion (see the Supporting Information).

A similar reaction, incorporating the dbm ligand (Hdbm = dibenzoylmethane) in place of dpm, in the absence of carboxylic acid, that is, solvothermal reaction of $[\text{Co}(\text{dbm})_2(\text{H}_2\text{O})_2]$ with H_3cht (1:1) in EtOH at 150°C , gives $[\text{Co}_{19}\text{O}_2(\text{OH})_2(\text{dbm})_6(\text{cht})_6(\text{Hcht})_2(\text{PhCO}_2)_4(\text{EtOH})_2]\cdot\text{H}_2\text{O}$ (**3**; 26 %) as orange crystals.^[11] Cluster **3** consists of two identical supertetrahedral subunits sharing the Co1 vertex (Figure 3). The subunits are similar to those for **1** and **2**, with diketonates chelating the unshared vertices (Co3, Co8, and Co10) and, as in **2**, the faces are capped by (three) 6.333-bound $(\text{cht})^{3-}$ ligands and (one) 5.331-bound $(\text{Hcht})^{2-}$ ligand (Figure 2c). The latter is on the face of Co3, Co8, and Co10. This face is also bound by a μ_3 hydroxide (through Co4, Co9,

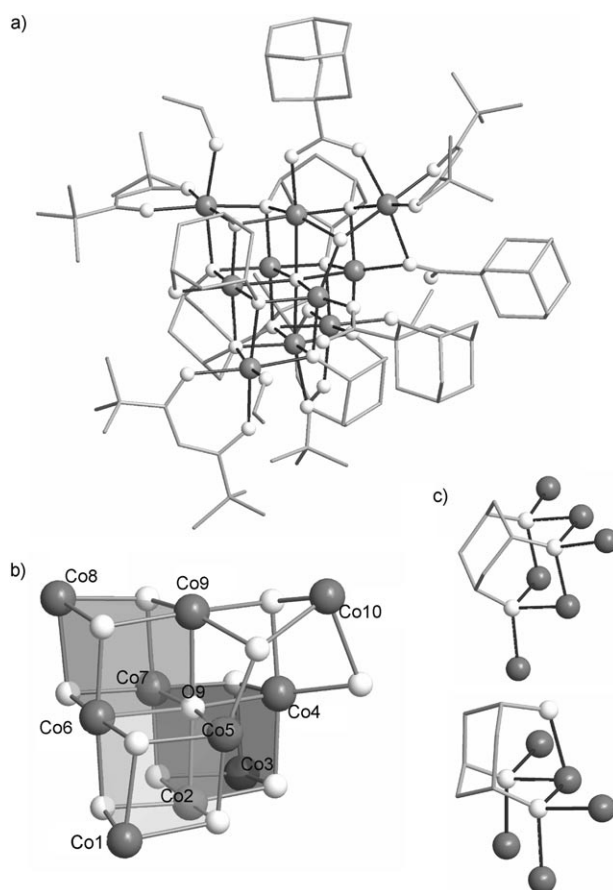


Figure 2. a) Structure of **2** in the crystal; b) view of the inorganic core; c) the 6.333 (top) and 5.331 (bottom) binding modes for the $(\text{H}_3-x)\text{cht}$ ligands.

and Co10). One $\{\text{Co}_4\text{O}_4\}$ cubane unit in each subunit has an elongated edge (Co3–O5 2.599 Å; Figure 3b). Two benzoate groups, arising from degradation of the diketonate ligands,^[4] bridge the Co3–Co4 and Co8–Co9 edges. Co10 is coordinated to a terminal solvent molecule. Co2, Co5, and Co6 are five-coordinate. BVS and charge balance support the presence of nineteen Co^{II} ions (see Supporting Information).

These results show the sensitivity of this cobalt coordination chemistry to minor changes in reaction conditions, leading to very different, but clearly related, structures, in stark contrast to the much more robust $[\text{Ni}^{\text{II}}(\text{diketonate})_2]$ -triol solvothermal reaction system,^[4] which can accommodate a range of triols (stoichiometric or excess; the cobalt system requires an excess), carboxylates, and diketonates, in alcohol or nitrile solvents, to give a variety of $\{\text{Ni}_{10}\}$ species, all with the symmetrical $\{\text{Ni}_{10}\text{O}(\text{L})_4(\text{diketonate})_4\}$ core (L = fully deprotonated triol). The first examples of such a system were $[\text{Ni}_{10}\text{O}(\text{thme})_4(\text{dbm})_4(\text{O}_2\text{CPh})_2(\text{EtOH})_6]$ (H_3thme = 1,1,1-tris(hydroxymethyl)ethane) and $[\text{Ni}_{10}\text{O}(\text{cht})_4(\text{dpm})_4(\text{O}_2\text{CMe})_2(\text{H}_2\text{O})_2]$, the latter incorporating the constrained cyclohexanetriol as a tridentate face-capping ligand, in contrast to the analogous cobalt chemistry, wherein the constrained triol leads to the ruptured $\{\text{Co}_{10}\}$ cluster **2** or the bi-supertetrahedral $\{\text{Co}_{19}\}$ cluster **3**.

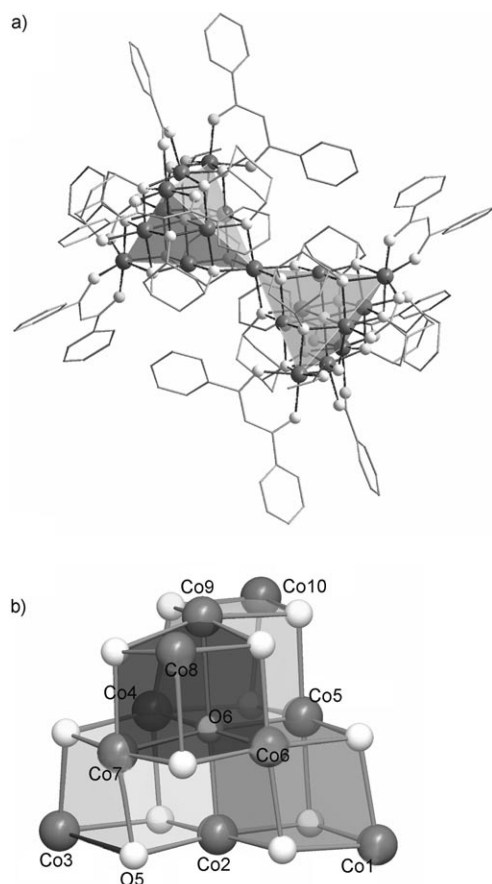


Figure 3. a) The structure of **3** in the crystal, highlighting the vertex-sharing bi-supertetrahedron; b) the inorganic subunit.

Preliminary studies have shown that the symmetrical supertetrahedral cluster **1** exhibits slow magnetization dynamics:^[3] a field-dependent maximum in molar magnetic susceptibility $\chi_M T(T)$, at 12 K (Figure 4a) below which temperature there is a divergence of field-cooled (FC) and zero-field-cooled (ZFC) magnetization curves (Figure 4a, inset), and a small frequency-dependence of the low-temperature ac susceptibility with a peculiar peak in the out-of-phase component $\chi''_{ac}(T)$ showing a maximum at a temperature that is essentially independent of frequency (Figure 5a). The latter contrasts with typical SMM behavior. Slow magnetization dynamics are further evidenced by the opening of a hysteresis loop in the magnetization versus the applied field (see the Supporting Information) and magnetization retention over several hours after field-cooling (Figure 5b). Interestingly, this behavior does not occur in the opened supertetrahedral cage **2**. In this case, $\chi_M T(T)$ decreases continuously with decreasing T , there is no opening of FC/ZFC curves (Figure 4b), and there is no peak in the $\chi''_{ac}(T)$ signal down to 1.8 K. Notably, the very similar reaction conditions for **1** and **2** (and **3**) suggest no extrinsic (impurity) origin for the unusual magnetic behavior of **1**. Also, there are no covalent links nor any other apparent pathway for exchange between molecules through the aliphatic ligands (see the Supporting Information, Figure S3; shortest intermolecular Co...Co distances in **1** and **2** are approximately 10.5 Å and 9.0 Å, respectively).^[13] More-

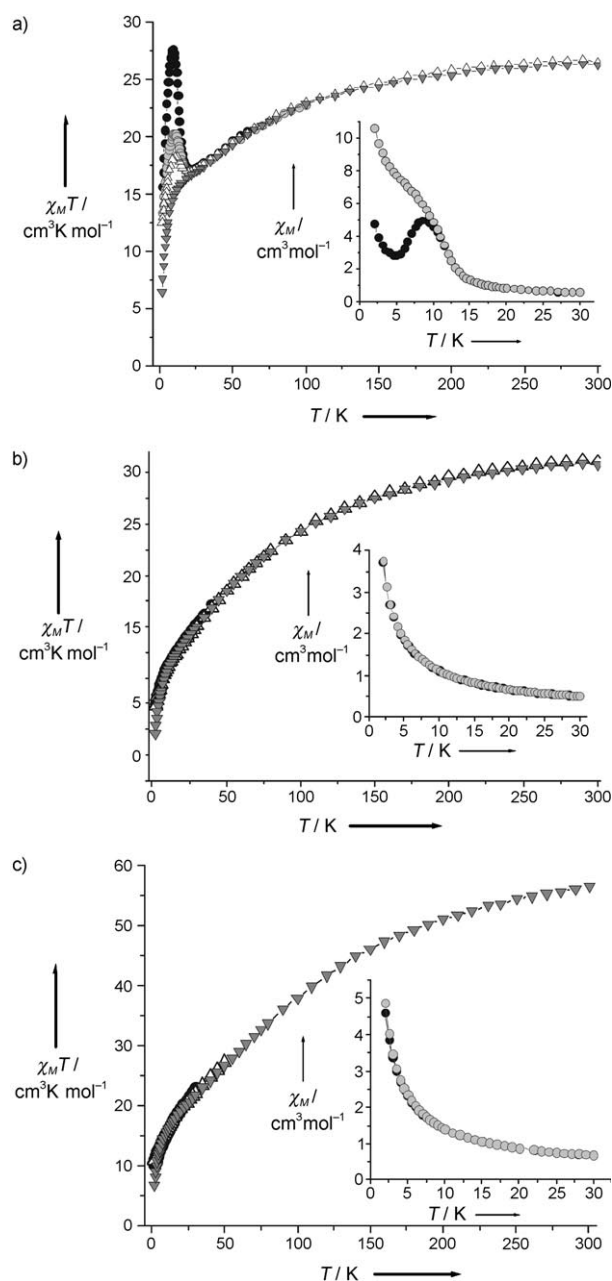


Figure 4. $\chi_M T$ versus T measured in 1 T (∇), 0.1 T (Δ), 0.05 T (\bullet), or 0.01 T (\circ) applied fields for a) **1**, b) **2**, and c) **3**. Insets: field-cooled (\bullet) and zero-field-cooled (\circ) curves measured in 0.01 T applied fields.

over, the only disorder in the structure of **1** is in the positions of a methanol ligand and a μ -carboxylate ligand on one edge of the supertetrahedron. As both intermolecular coupling and disorder are considered essential factors supporting spin-glass behavior, we are led to rule this behavior out for **1**, as in the case of $[\text{Ni}_{10}]$. For **3**, $\chi_M T$ has approximately double the room-temperature value for **1** and **2**, decreasing continuously with decreasing T (Figure 4c). No divergence occurs in FC or ZFC curves down to 2 K, although there is a significant rise in $\chi''_{ac}(T)$ at temperatures approaching 2 K (see the Supporting Information). Lower temperature measurements are required before any meaningful conclusion can be made for **3**.

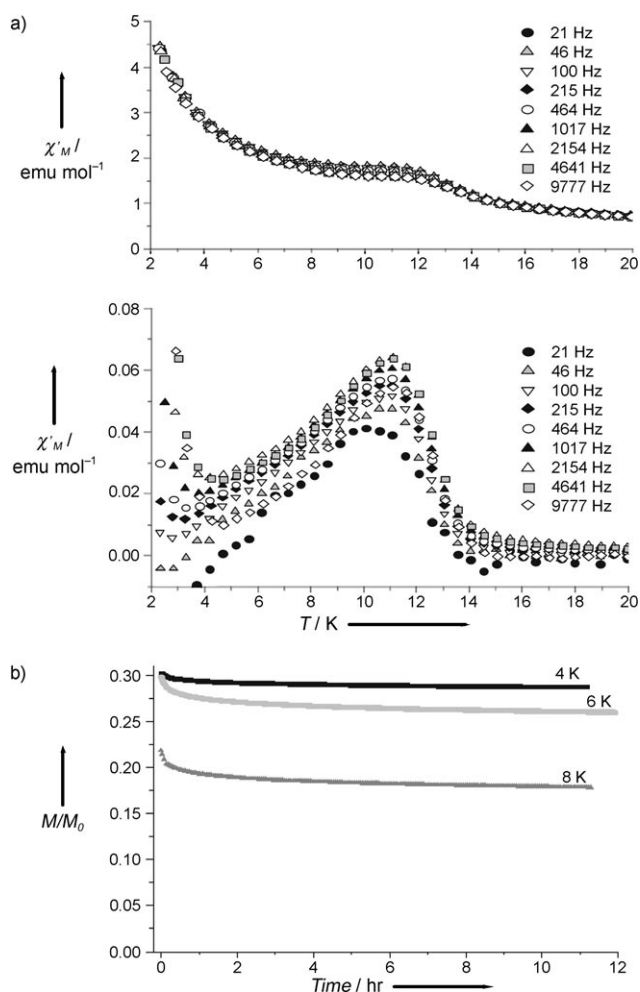


Figure 5. a) In-phase (top) and out-of-phase (bottom) magnetic susceptibility of **1** measured from 21 to 9777 Hz under a 10 Oe oscillating field; b) dc relaxation data for **1** at 4, 6, and 8 K plotted as M/M_0 versus time where M_0 is the magnetization value before starting the decay and after cooling the sample in a 0.01 T applied field.

Unfortunately, the orbital magnetic moment of the octahedral Co^{II} ion has so far precluded quantitative analysis.

In summary, in complex **1** we have detected slow magnetic relaxation at temperatures up to 12 K, much higher than those for SMMs to date. The similarity in the behavior of $\{\text{Ni}_{10}\}$ and **1**, but not **2**, supports the association of unusual magnetic phenomena with the regular supertetrahedral $\{\text{M}_{10}\}$ structure, supporting the model proposed in reference [3], only the second example of this phenomenon. We note that unusual frustration effects have been predicted for other high-symmetry deltahedral clusters, such as Müller's icosidodecahedral $\{\text{Mo}_{72}\text{Fe}_{30}\}$ Keplerate.^[14] Detailed low-temperature measurements on **1–3** are in progress. The versatility of this simple reaction system holds great promise for the development of Co^{II} cluster chemistry, which is less well-developed than that of other first row ions, but has been receiving increasing attention.^[8–10] In fact the enneadecametallate **3** is the second largest Co^{II} cluster isolated to date.^[15] Systematic exploration of the variable synthetic parameters is currently underway.

Experimental Section

$[\text{Co}(\text{diketonate})_2(\text{H}_2\text{O})_2]$ precursors were prepared according to literature procedures^[16] for the nickel(II) analogues (90 %). Elemental analysis calcd (%) for $\text{C}_{30}\text{H}_{26}\text{CoO}_6$ ($[\text{Co}(\text{dbm})_2(\text{H}_2\text{O})_2]$): Co 10.88, C 66.54, H 4.83; found: Co 10.90, C 66.33, H 4.64. Calcd (%) for $\text{C}_{22}\text{H}_{42}\text{CoO}_6$ ($[\text{Co}(\text{dpm})_2(\text{H}_2\text{O})_2]$): Co 12.76, C 57.25, H 9.17; found: Co 12.77, C 56.64, H 8.98.

1: $[\text{Co}(\text{dpm})_2(\text{H}_2\text{O})_2]$ (0.25 g, 0.54 mmol), H_3tmp (0.073 g, 0.54 mmol), and AdCO_2H (0.097 g, 0.54 mmol) in MeOH (9 mL) were heated at 150 °C for 12 h in a teflon-lined autoclave. After slow cooling (1°C min^{-1}) to room temperature, brown crystals of **1** were collected, washed by sonication in MeOH, and dried in air (0.068 g, 51 % based on Co). Elemental analysis calcd (%) for $\text{C}_{99}\text{H}_{175}\text{Co}_{10}\text{O}_{31}$: Co 24.04, C 48.51, H 7.19; found: Co 23.78, C 48.05, H 7.09.

2: $[\text{Co}(\text{dpm})_2(\text{H}_2\text{O})_2]$ (0.25 g, 0.54 mmol), H_3cht (0.091 g, 0.54 mmol), and AdCO_2H (0.097 g, 0.54 mmol) in EtOH (4 mL) were heated at 150 °C for 12 h as above. After slow cooling (1°C min^{-1}) to room temperature, purple crystals of **2** were collected, washed by sonication in EtOH, and dried in air (0.092 g, 66 %). Elemental analysis calcd (%) for $\text{C}_{107}\text{H}_{178}\text{Co}_{10}\text{O}_{31}$: Co 23.11, C 50.40, H 7.03; found: Co 23.16, C 49.72, H 6.97.

3: $[\text{Co}(\text{dbm})_2(\text{H}_2\text{O})_2]$ (0.29 g, 0.54 mmol) and H_3cht (0.091 g, 0.54 mmol) in EtOH (9 mL) were heated at 150 °C for 12 h as above. After slow cooling ($0.5^\circ\text{C min}^{-1}$) to room temperature, orange crystals of **3** were collected, washed by sonication in EtOH, and dried in air (0.031 g, 26 %). Elemental analysis calcd (%) for $\text{C}_{170}\text{H}_{176}\text{Co}_{19}\text{O}_{51}$: Co 26.94, C 49.14, H 4.26; found: Co 27.23, C 48.09, H 4.01.

Magnetic measurements were performed on a Quantum Design MPMS SQUID magnetometer on polycrystalline samples restrained in eicosane. Data were corrected for the diamagnetism of the samples using Pascal constants, and the sample holder by measurement. Frequency-dependent ac-susceptibility measurements used a QD-PPMS ACMS option. Sample purity was additionally confirmed by powder X-ray diffraction.

Received: August 22, 2008

Keywords: cluster compounds · cobalt · magnetic properties · solvothermal synthesis

- [1] a) D. Gatteschi, R. Sessoli, *Angew. Chem.* **2003**, *115*, 278; *Angew. Chem. Int. Ed.* **2003**, *42*, 268; b) D. Gatteschi, R. Sessoli, J. Villain, *Molecular Nanomagnets*, Oxford University Press, New York, **2006**, and references therein.
- [2] C. J. Milios, A. Vinslava, W. Wernsdorfer, S. Moggach, S. P. Perlepes, G. Christou, E. K. Brechin, *J. Am. Chem. Soc.* **2007**, *129*, 2754.
- [3] S. Carretta, P. Santini, G. Amoretti, M. Affronte, A. Candini, A. Ghirri, I. S. Tidmarsh, R. H. Laye, R. Shaw, E. J. L. McInnes, *Phys. Rev. Lett.* **2006**, *97*, 207201.
- [4] R. Shaw, I. S. Tidmarsh, R. H. Laye, B. Breeze, M. Helliwell, E. K. Brechin, S. L. Heath, M. Murrie, S. Ochsenbein, H.-U. Güdel, E. J. L. McInnes, *Chem. Commun.* **2004**, 1418.
- [5] a) M. I. Khan, J. Zubieta, *Prog. Inorg. Chem.* **1995**, *43*, 1; b) A. Müller, J. Meyer, H. Bogge, A. Stämmler, A. Botar, *Chem. Eur. J.* **1998**, *4*, 1388; c) E. K. Brechin, *Chem. Commun.* **2005**, 5141.
- [6] P. W. Anderson, *Phys. Rev.* **1959**, *114*, 1002.
- [7] Supertetrahedral $\{\text{Mn}_{10}\}$ and bi-supertetrahedral $\{\text{Mn}_{19}\}$ cages are known, but these lack central μ_6 oxides and are fully ferromagnetically coupled: a) T. C. Stammatos, K. A. Abboud, W. Wernsdorfer, G. Christou, *Angew. Chem.* **2006**, *118*, 4240; *Angew. Chem. Int. Ed.* **2006**, *45*, 4134; b) A. M. Ako, I. J. Hewitt, V. Mereacre, R. Clérac, W. Wernsdorfer, C. E. Anson, A. K. Powell, *Angew. Chem.* **2006**, *118*, 5048; *Angew. Chem. Int. Ed.*

- 2006, 45, 4926; c) M. Manoli, R. D. L. Johnstone, S. Parsons, M. Murrie, M. Affronte, M. Evangelisti, E. K. Brechin, *Angew. Chem. Int. Ed.* **2007**, 46, 4456.
- [8] a) A. Tsohos, S. Dionyssopoulou, C. P. Raptopoulou, A. Terzis, E. G. Bakalbassis, *Angew. Chem. Int. Ed.* **1999**, 38, 983; b) G. S. Papaefstathiou, A. Escuer, R. Vicente, M. Font-Bardia, X. Solans, S. P. Perlepes, *Chem. Commun.* **2001**, 2414.
- [9] a) A. J. Blake, C. M. Grant, S. Parsons, J. M. Rawson, R. E. P. Winpenny, *J. Chem. Soc. Chem. Commun.* **1994**, 2363; b) E. K. Brechin, O. Cador, A. Caneschi, C. Cadiou, S. G. Harris, S. Parsons, M. Vonci, R. E. P. Winpenny, *Chem. Commun.* **2002**, 1860.
- [10] G. J. T. Cooper, G. N. Newton, P. Kögerler, D.-L. Long, L. Engelhardt, M. Luban, L. Cronin, *Angew. Chem. Int. Ed.* **2007**, 46, 1340.
- [11] Crystal data for **1** ($\text{C}_{99}\text{H}_{156}\text{Co}_{10}\text{O}_{31}$): brown needle, monoclinic, space group $C2/c$, $a = 31.182(3)$, $b = 18.3994(19)$, $c = 25.424(3)$ Å, $\beta = 125.466(2)^\circ$, $V = 11880(2)$ Å³, $Z = 4$, $T = 100(2)$ K, $\rho = 1.359$ g cm⁻³, $F(000) = 5072$, $\mu(\text{Mo}_{\text{K}\alpha}) = 1.426$ mm⁻¹; $wR_2 = 0.2902$ (12119 unique reflections), $R_1 = 0.0952$ (5205 reflections with $I > 2\sigma(I)$), GOF = 1.050. Crystal data for **2** ($\text{C}_{107}\text{H}_{178}\text{Co}_{10}\text{O}_{31}$): purple parallelepiped, triclinic, space group $P\bar{1}$, $a = 15.557(8)$, $b = 16.383(8)$, $c = 23.788(12)$ Å, $\alpha = 83.645(10)$, $\beta = 82.700(9)$, $\gamma = 75.693(9)^\circ$, $V = 5807(5)$ Å³, $Z = 2$, $T = 150(2)$ K, $\rho = 1.458$ g cm⁻³, $F(000) = 2676$, $\mu(\text{Mo}_{\text{K}\alpha}) = 1.462$ mm⁻¹; $wR_2 = 0.2439$ (16543 unique reflections), $R_1 = 0.1032$ (9346 reflections with $I > 2\sigma(I)$), GOF = 1.022. Crystal data for **3** ($\text{C}_{170}\text{H}_{158}\text{Co}_{19}\text{O}_{51}$): orange plate, triclinic, space group $P\bar{1}$, $a = 14.9391(7)$, $b = 15.5500(7)$, $c = 20.4855(9)$ Å, $\alpha = 75.8260(10)$, $\beta = 72.6620(10)$, $\gamma = 63.2120(10)^\circ$, $V = 4020.8(3)$ Å³, $Z = 1$, $T = 150(2)$ K, $\rho = 1.708$ g cm⁻³, $F(000) = 2099$, $\mu(\text{Mo}_{\text{K}\alpha}) = 1.987$ mm⁻¹; $wR_2 = 0.1150$ (14677 unique reflections), $R_1 = 0.0444$ (11914 reflections with $I > 2\sigma(I)$), GOF = 1.024. Crystals of **1** and **2** are poorly diffracting and, despite numerous efforts, the best data sets obtained still give large reliability factors. Data were collected on a Bruker SMART CCD diffractometer for **1** and **2** ($\text{Mo}_{\text{K}\alpha}$, $\lambda = 0.71069$ Å), and on a Bruker APEX II CCD diffractometer for **3** (synchrotron, $\lambda = 0.6710$ Å). Crystals were mounted on a Hamilton cryoloop (**1** and **2**) or on the tip of a glass pin (**3**) using Paratone-N oil and placed in the cold flow produced with an Oxford Cryocooling device. Complete hemispheres of data were collected using ω scans (0.3° , 30 s/frame for **1**, 10 s/frame for **2** and 0.36° , 1 s/frame for **3**). Integrated intensities were obtained with SAINT+ and were corrected for absorption with SADABS; structure solution and refinement was performed with the SHELXTL-package.^[17] The structures were solved by direct methods and completed by iterative cycles of ΔF syntheses and full-matrix least-squares refinement against F^2 . CCDC 693424, 693425, and 693426 contain the supplementary crystallographic data for this paper. These data can be obtained free of charge from The Cambridge Crystallographic Data Centre via www.ccdc.cam.ac.uk/data_request/cif.
- [12] R. A. Coxall, S. G. Harris, D. K. Henderson, S. Parsons, P. A. Tasker, R. E. P. Winpenny, *J. Chem. Soc. Dalton Trans.* **2000**, 2349.
- [13] Long range magnetic ordering is ruled out by the lack of any evident anomaly in specific heat data.
- [14] a) C. Schröder, H. Nojiri, J. Schnack, P. Hage, M. Luban, P. Kögerler, *Phys. Rev. Lett.* **2005**, 94, 107205; b) A. Müller, S. Sarkar, S. Q. N. Shah, H. Bögge, M. Schmidtman, S. Sarkar, P. Kögerler, B. Hauptfleisch, A. X. Trautwein, V. Schunemann, *Angew. Chem.* **1999**, 111, 3435; *Angew. Chem. Int. Ed.* **1999**, 38, 3238.
- [15] E. K. Brechin, S. G. Harris, A. Harrison, S. Parsons, G. A. Whittaker, R. E. P. Winpenny, *Chem. Commun.* **1997**, 653.
- [16] a) M. J. Collins, H. F. Henneke, *Inorg. Chem.* **1973**, 12, 2983; b) D. V. Soldatov, A. T. Henegouwen, G. D. Enright, C. I. Ratcliffe, J. A. Ripmeester, *Inorg. Chem.* **2001**, 40, 1626.
- [17] SHELXTL-PC Package. Bruker Analytical X-ray Systems: Madison, WI, **1998**.